

# Melt Polymerization of Bisphenol-A and Diphenyl Carbonate in a Semibatch Reactor

BOO-GON WOO,<sup>1</sup> KYU YONG CHOI,<sup>1</sup> KWANG HO SONG,<sup>2</sup> SANG HO LEE<sup>2,3</sup>

<sup>1</sup> Department of Chemical Engineering, University of Maryland, College Park, Maryland 20742

<sup>2</sup> LG Chem Research Park, LG Chemical Company, Taejon, South Korea

<sup>3</sup> Donga University, Pusan, South Korea

Received 20 January 2000; accepted 7 August 2000

**ABSTRACT:** The effect of thermodynamic phase equilibrium on the kinetics of semibatch melt polycondensation of bisphenol-A and diphenyl carbonate was studied for the synthesis of polycarbonate. In the melt-polymerization process, a partial loss of diphenyl carbonate occurs as the reaction by-product phenol is removed from the reactor. To obtain a high molecular weight polymer under high temperature and low-pressure conditions, a stoichiometric mol ratio of the two reactive end groups needs to be maintained during the polymerization. In this work, vapor-liquid equilibrium data for a binary mixture of phenol and diphenyl carbonate are reported and they are used in conjunction with the Wilson equation to calculate the exact amounts of diphenyl carbonate and phenol returned from a reflux column to the reactor. A good agreement between the reactor model simulations and the experimental polymerization data was obtained. It was also observed that diphenyl carbonate is quickly consumed during the early stage of polymerization and the fraction of evaporated diphenyl carbonate refluxed to the reactor is essentially constant during this period. © 2001 John Wiley & Sons, Inc. *J Appl Polym Sci* 80: 1253–1266, 2001

**Key words:** polycarbonate; melt polymerization; vapor-liquid equilibrium; semibatch polymerization; polymerization modeling

## INTRODUCTION

Polycarbonate (PC) is one of the most rapidly growing thermoplastic engineering polymers with high heat resistance, impact resistance, optical clarity, and dimensional stability.<sup>1</sup> Polycarbonate is used in many applications such as in nursing bottles, data-storage devices, and structural ma-

terials for electrical and electronic applications, automobiles, and construction applications.<sup>2</sup> The global demand of polycarbonates has been growing more than 10% per year.<sup>1</sup> This growth rate has been a driving factor for the increase in global production capacity of polycarbonates, which is now about 1 million tons per year.

Polycarbonate is manufactured industrially by an interfacial phosgenation process and by a melt-transesterification process. The melt process is environmentally more benign than is the interfacial phosgenation process and, hence, attracting more industrial interest in recent years. In a typ-

---

Correspondence to: K. Y. Choi.  
Contract grant sponsor: LG Chemical Co., Taejon, South Korea.

*Journal of Applied Polymer Science*, Vol. 80, 1253–1266 (2001)  
© 2001 John Wiley & Sons, Inc.

ical melt-transesterification process, diphenyl carbonate (DPC) and bisphenol-A (BPA: 4,4-dihydroxydiphenyl 2,2-propane) are polymerized in the presence of a catalyst such as lithium hydroxide. The transesterification is a reversible reaction and the reaction by-product (phenol) must be distilled off continuously to facilitate the forward chain-growth reaction. Phenol is removed from the melt phase by applying a high vacuum. As the polymer molecular weight increases, the melt viscosity increases rapidly and, hence, the polymerization becomes mass transfer-controlled. Therefore, the melt-polymerization process requires specially designed reactor equipment providing large mass-transfer interfacial areas to deal with a highly viscous polymer melt under high temperature (280–300°C) and vacuum conditions to obtain high molecular weight polycarbonate.

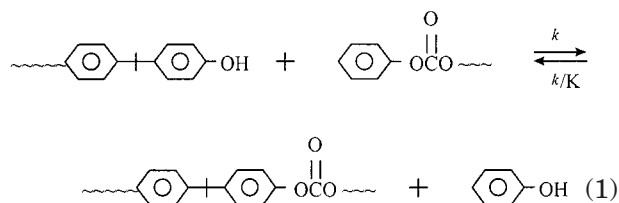
As phenol vapor is removed from the melt-polymerization reactor, some DPC is also removed from the reactor because DPC exhibits moderate vapor pressure at the reaction temperature. Any loss of DPC during the reaction will cause significant variations in the concentration of reactive end groups (phenyl carbonate and hydroxyl groups) that, in turn, will make high molecular weight polymers difficult to obtain. Therefore, it is important to keep the stoichiometric ratio of the two functional end groups during the course of polymerization. To do so, an appropriate initial DPC/BPC mol ratio needs to be employed to compensate for the loss of DPC in a reflux column.

In our previous work,<sup>3</sup> a detailed reactor model was developed to investigate multistage polycondensation in a semibatch reactor. To account for the loss of DPC in a reflux column, an empirical reflux efficiency factor was introduced. The reflux efficiency factor is defined as the molar fraction of evaporated DPC that is refluxed back to the reactor in condensed form. The reflux efficiency factor was adjusted to fit the experimentally measured molecular weight data.

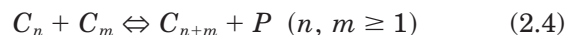
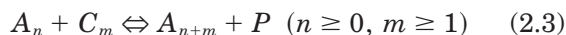
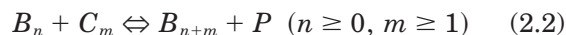
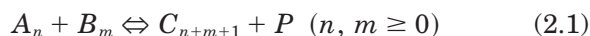
In this article, we present a new method to calculate the exact amount of condensed DPC refluxed back to the reactor using vapor–liquid equilibrium data for the DPC–phenol system. This method eliminates the use of an empirical reflux efficiency factor for the simulation of semibatch polymerization of BPA polycarbonate.

## REACTION MODEL

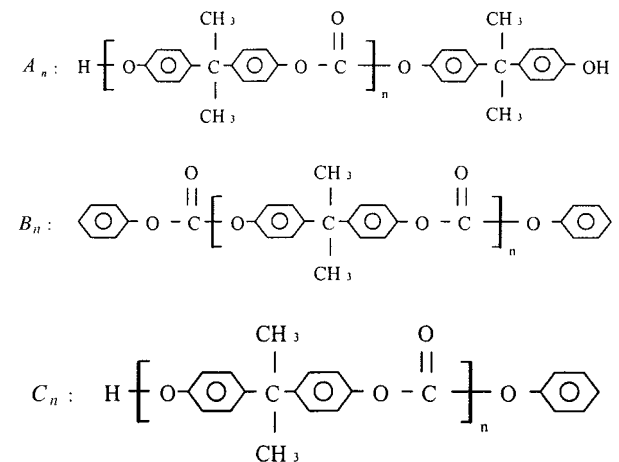
The melt transesterification of DPC and BPA occurs between the hydroxyl end group in BPA and the phenyl carbonate end group in DPC in the presence of a catalyst (e.g., lithium hydroxide):



For the modeling of a batch or a semibatch melt-transesterification process, either a functional group model or a molecular species model can be used. With the functional group model, the overall conversion of reactive end groups in the reaction mixture can be easily calculated. In the current system, where one of the monomers evaporates during the reaction, the molecular species model is more convenient to calculate the variations in the monomer concentrations and the molecular weight of oligomers and polymers. Therefore, we shall use a molecular species model in which the transesterification reactions are represented as follows<sup>3</sup>:



where  $P$  is phenol and the three polymeric species ( $A_n$ ,  $B_n$ , and  $C_n$ ) are defined as



The mass-balance equations for the monomers and polymeric species and the molecular weight moment equations takes the following form:

$$V \frac{dA_0}{dt} = k(-4A_0B_0 - 4A_0\lambda_{B,0} - 2A_0\lambda_{C,0}) + k'(P\lambda_{C,0} + 2P\lambda_{A,0}) \quad (3)$$

$$V \frac{dB_0}{dt} = k(-4A_0B_0 - 4B_0\lambda_{A,0} - 2B_0\lambda_{C,0}) + k'(P\lambda_{C,0} + 2P\lambda_{B,0}) \quad (4)$$

$$V \frac{dP}{dt} = k[4A_0B_0 + 4A_0\lambda_{B,0} + 4B_0\lambda_{A,0} + 4\lambda_{A,0}\lambda_{B,0} + 2A_0\lambda_{C,0} + 2\lambda_{A,0}\lambda_{C,0} + 2B_0\lambda_{C,0} + 2\lambda_{B,0}\lambda_{C,0} + (\lambda_{C,0})^2] + k'[-2P\lambda_{C,1} - 2P\lambda_{A,1} - 2P\lambda_{B,1} + P\lambda_{C,0}] \quad (5)$$

$$V \frac{d\lambda_{A,0}}{dt} = k(-4B_0\lambda_{A,0} - 4\lambda_{A,0}\lambda_{B,0} + 2A_0\lambda_{C,0}) + k'(P\lambda_{C,1} - P\lambda_{C,0} - 2P\lambda_{A,0}) \quad (6)$$

$$V \frac{d\lambda_{B,0}}{dt} = k(-4A_0\lambda_{B,0} - 4\lambda_{A,0}\lambda_{B,0} + 2B_0\lambda_{C,0}) + k'(P\lambda_{C,1} - P\lambda_{C,0} - 2P\lambda_{B,0}) \quad (7)$$

$$V \frac{d\lambda_{C,0}}{dt} = k \times \left[ \begin{array}{l} 4A_0B_0 + 4A_0\lambda_{B,0} + 4\lambda_{A,0}B_0 + 4\lambda_{A,0}\lambda_{B,0} \\ - 2A_0\lambda_{C,0} - 2\lambda_{A,0}\lambda_{C,0} \\ - 2B_0\lambda_{C,0} - 2\lambda_{B,0}\lambda_{C,0} - (\lambda_{C,0})^2 \end{array} \right] + k'(-P\lambda_{C,0} + 2P\lambda_{A,1} + 2P\lambda_{B,1}) \quad (8)$$

$$V \frac{d\lambda_{A,1}}{dt} = k \times (-4B_0\lambda_{A,1} - 4\lambda_{A,1}\lambda_{B,0} + 2A_0\lambda_{C,1} + 2\lambda_{A,0}\lambda_{C,1}) + k' \left( \frac{1}{2}P\lambda_{C,2} - \frac{1}{2}P\lambda_{C,1} - P\lambda_{A,2} - P\lambda_{A,1} \right) \quad (9)$$

$$V \frac{d\lambda_{B,1}}{dt} = k \times (-4A_0\lambda_{B,1} - 4\lambda_{B,1}\lambda_{A,0} + 2B_0\lambda_{C,1} + 2\lambda_{B,0}\lambda_{C,1}) + k' \left( \frac{1}{2}P\lambda_{C,2} - \frac{1}{2}P\lambda_{C,1} - P\lambda_{B,2} - P\lambda_{B,1} \right) \quad (10)$$

$$V \frac{d\lambda_{C,1}}{dt} = k \times \left( \begin{array}{l} 4A_0B_0 + 4A_0\lambda_{B,1} + 4A_0\lambda_{B,0} + 4B_0\lambda_{A,0} \\ + 4B_0\lambda_{A,1} + 4\lambda_{A,1}\lambda_{B,0} + 4\lambda_{A,0}\lambda_{B,1} + A\lambda_{A,0}\lambda_{B,0} \\ - 2A_0\lambda_{C,1} - 2\lambda_{A,0}\lambda_{C,1} - 2B_0\lambda_{C,1} - 2\lambda_{B,0}\lambda_{C,1} \end{array} \right) + k'(P\lambda_{B,1} - P\lambda_{C,2} + P\lambda_{A,1} + P\lambda_{B,2} + P\lambda_{A,2}) \quad (11)$$

$$V \frac{d\lambda_{A,2}}{dt} = k(-4B_0\lambda_{A,2} - 4\lambda_{A,2}\lambda_{B,0} + 2A_0\lambda_{C,2} + 4\lambda_{A,1}\lambda_{C,1} + 2\lambda_{A,0}\lambda_{C,2}) + k' \left( \frac{1}{3}P\lambda_{C,3} - \frac{1}{2}P\lambda_{C,2} + \frac{1}{6}P\lambda_{C,1} - \frac{4}{3}P\lambda_{A,3} - P\lambda_{A,2} + \frac{1}{3}P\lambda_{A,1} \right) \quad (12)$$

$$V \frac{d\lambda_{B,2}}{dt} = k(-4A_0\lambda_{B,2} - 4\lambda_{B,2}\lambda_{A,0} + 2B_0\lambda_{C,2} + 4\lambda_{B,1}\lambda_{C,1} + 2\lambda_{B,0}\lambda_{C,2}) + k' \left( \frac{1}{3}P\lambda_{C,3} - \frac{1}{2}P\lambda_{C,2} + \frac{1}{6}P\lambda_{C,1} - \frac{4}{3}P\lambda_{B,3} - P\lambda_{B,2} + \frac{1}{3}P\lambda_{B,1} \right) \quad (13)$$

$$V \frac{d\lambda_{C,2}}{dt} = k \left[ \begin{array}{l} 4A_0B_0 + 4A_0\lambda_{B,2} + 8A_0\lambda_{B,1} + 4A_0\lambda_{B,0} + 4\lambda_{A,2}B_0 + 4\lambda_{A,2}\lambda_{B,0} \\ + 8\lambda_{A,1}B_0 + 8\lambda_{A,1}\lambda_{B,1} + 8\lambda_{A,1}\lambda_{B,0} + 4\lambda_{A,0}B_0 + 4\lambda_{A,0}\lambda_{B,2} + 8\lambda_{A,0}\lambda_{B,1} \\ + 4\lambda_{A,0}\lambda_{B,0} - 2A_0\lambda_{C,2} - 2\lambda_{A,0}\lambda_{C,2} - 2B_0\lambda_{C,2} - 2\lambda_{B,0}\lambda_{C,2} + 2(\lambda_{C,1})^2 \end{array} \right] + k' \left( \begin{array}{l} \frac{2}{3}P\lambda_{A,3} + P\lambda_{A,2} + \frac{1}{3}P\lambda_{A,1} + \frac{2}{3}P\lambda_{B,3} + P\lambda_{B,2} + \frac{1}{3}P\lambda_{B,1} - \\ \frac{4}{3}P\lambda_{C,3} + \frac{1}{3}P\lambda_{C,1} \end{array} \right) \quad (14)$$

In the above,  $V$  is the reaction volume and all the dependent variables are in moles. The  $k$ -th molecular weight moments for  $A_n$ ,  $B_n$ , and  $C_n$  polymeric species are defined as

$$\lambda_{A,k} = \sum_{n=1}^{\infty} n^k A_n, \quad \lambda_{B,k} = \sum_{n=1}^{\infty} n^k B_n, \quad \lambda_{C,k} = \sum_{n=1}^{\infty} n^k C_n \quad (15)$$

The third moment is dependent on the lower-order molecular weight moments and the following moment closure formula is used:

$$\lambda_{i,3} = \frac{\lambda_{i,2}(2\lambda_{i,2}\lambda_{i,0} - \lambda_{i,1}^2)}{\lambda_{i,1}\lambda_{i,0}} \quad (i = A, B, C) \quad (16)$$

Then, the number-average molecular weight ( $M_n$ ) and the weight-average molecular weight ( $M_w$ ) are calculated as follows:

$$M_n = \frac{\sum_{n=1}^{\infty} (A_n W_{A_n} + B_n W_{B_n} + C_n W_{C_n})}{\sum_{n=1}^{\infty} (A_n + B_n + C_n)} \quad (17)$$

$$M_w = \frac{\sum_{n=1}^{\infty} (A_n W_{A_n}^2 + B_n W_{B_n}^2 + C_n W_{C_n}^2)}{\sum_{n=1}^{\infty} (A_n W_{A_n} + B_n W_{B_n} + C_n W_{C_n})} \quad (18)$$

where the molecular weight of each species is

$$W_{A_n} = (254.3)n + 228.29 \quad (19.1)$$

$$W_{B_n} = (254.3)n + 214.22 \quad (19.2)$$

$$W_{C_n} = (254.3)n + 94.11 \quad (19.3)$$

In the above equations, the contribution of each end group to the molecular weight of each polymeric species was accounted for. This end-group effect should be included in calculating the molecular weight of low molecular weight polymers, particularly in the prepolymerization stage.

The rate constants in the above model are the effective rate constants in which the catalyst con-

centration effect is incorporated. Since the transesterification reaction occurs to some extent even without any catalyst, the rate constant of the following form is used<sup>3</sup>:

$$k = k_u + k_c[C^*] \quad (20)$$

where  $[C^*]$  is the catalyst concentration (mol/L),  $k_u$  represents the rate constant for the uncatalyzed transesterification, and  $k_c$  represents the rate constant for the catalyzed transesterification.

The forward and reverse reaction rate constants for the uncatalyzed transesterification are

$$k_u = (3.108 \pm 0.102) \times 10^7 \exp[(-25,290 \pm 1,010)/RT] \quad \text{L mol}^{-1} \text{ min}^{-1} \quad (21.1)$$

$$k'_u = (2.028 \pm 0.226) \times 10^{15} \exp[(-45,030 \pm 2.430)/RT] \quad \text{L mol}^{-1} \text{ min}^{-1} \quad (21.2)$$

and for the catalyzed reactions:

$$k_c = 9.62 \times 10^8 \exp[-13900/RT] \quad \text{L}^2 \text{ mol}^{-2} \text{ min}^{-1} \quad (22.1)$$

$$k'_c = 8.04 \times 10^7 \exp[-12090/RT] \quad \text{L}^2 \text{ mol}^{-2} \text{ min}^{-1} \quad (22.2)$$

In the above rate constants, the activation energies are in cal/mol. Since the reaction volume decreases with conversion due to the removal of phenol and DPC, the reaction volume  $V$  is not constant. The computation procedure for the reaction volume can be found in ref. 3.

## EXPERIMENTAL

At high temperature ( $>200^\circ\text{C}$ ) and low pressure ( $<100$  mmHg), a significant amount of DPC can be lost from the reactor, particularly at the beginning of polymerization as pressure reduction is commenced. Thus, it is necessary to calculate the amount of DPC lost or refluxed during the course of polymerization. The main objectives of this work were first to obtain vapor-liquid equilibrium data for a binary mixture of phenol and DPC and to use them in the semibatch reactor model.

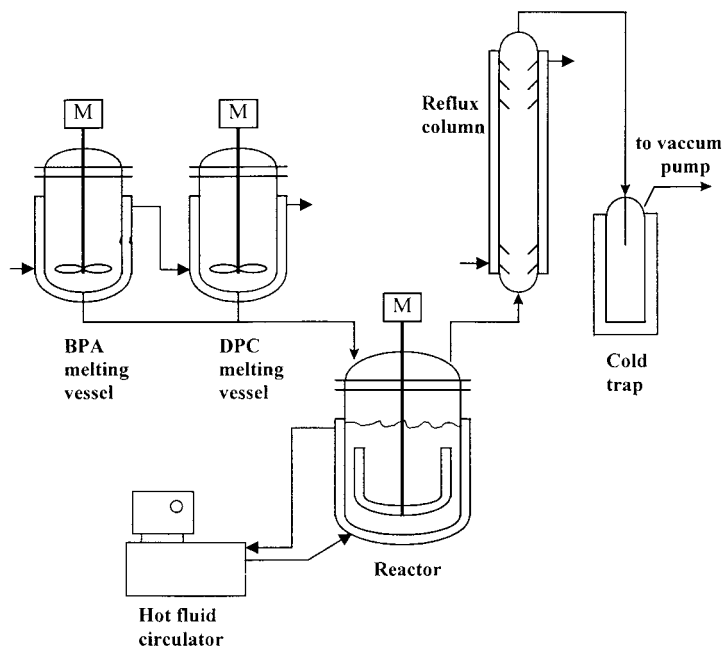


**Figure 1** Experimental semibatch reactor system for polycarbonate synthesis.

In this work, we assumed that BPA and the polymers are not volatile.

To obtain vapor–liquid equilibrium data for a phenol–DPC mixture, an experimental system that consists of a heated vessel and a condenser was assembled. To the heating vessel, predetermined amounts of phenol and DPC were added and the heating vessel was heated to a set-point temperature by circulating the heating oil in the vessel jacket. The mixture of phenol and the DPC vapor was condensed in the condenser. The condensed liquid was refluxed to the heating vessel until the system reached an equilibrium state. When the vapor–liquid equilibrium was established, the corresponding temperature was measured and small amounts of the samples were taken from both the heating vessel and the condensed liquid collector attached to the end of the condenser. The composition of each sample was analyzed by HPLC. This procedure was repeated for different phenol–DPC compositions.

For semibatch polymerization experiments, a stainless-steel jacketed reactor (volume, 4L) system illustrated schematically in Figure 1 was used. The DPC and BPA melting/supply vessels (2 L each) were heated and agitated. To supply these molten monomers, all the material transport lines were heated by an electrical wire. The temperature of the jacketed reflux column (Vigreux

type; length, 45.7 cm; diameter, 2.4 cm) was maintained constant by circulating hot oil at high flow rate. After molten DPC and BPA were charged to the reactor, a small amount of the catalyst ( $\text{LiOH} \cdot \text{H}_2\text{O}$ ) was injected into the reactor using a small syringe. A high vacuum ( $<10$  mmHg) was then applied to the system to remove the condensation by-product phenol. Recall that a small amount of DPC also evaporates with phenol.

### Compositions in Vapor and Liquid Phases

To solve the semibatch reactor model equations, the concentrations of phenol and DPC in both the vapor phase and the liquid phase need to be calculated. The following vapor pressure equations are used in this work for phenol and DPC<sup>4</sup>:

Phenol:

$$\log_{10} P_p^{\text{sat}} = 7.13 - \frac{1.52 \times 10^3}{T - 98.58} \quad (T \text{ in K}) \quad (23)$$

DPC:

$$\ln P_B^{\text{sat}} = \left( -\frac{1.48 \times 10^4}{1.987} \right) \cdot \frac{1}{T} + 19.55 \quad (T \text{ in K}) \quad (24)$$

$P_j^{\text{sat}}$  is the vapor pressure of component  $j$  in mmHg. If we assume that phenol and DPC in the vapor phase follow the ideal gas law, the partial pressure of the vapor species  $j$ ,  $p_j$ , is expressed as

$$p_j = p_t y_j = \gamma_j x_j P_j^{\text{sat}} \quad (25)$$

where  $p_t$  is the total pressure of the system;  $y_j$ , the mol fraction of component  $j$  in the vapor phase;  $\gamma_j$ , the activity coefficient of component  $j$ ; and  $x_j$ , the mol fraction of component  $j$  in the liquid phase.

To calculate the activity coefficient, the Flory–Huggins equation is used<sup>5</sup>:

$$\ln \gamma_j = \ln \left[ 1 - \left( 1 - \frac{1}{m_j} \right) (1 - \Phi_j) \right] + \left( 1 - \frac{1}{m_j} \right) (1 - \Phi_j) + \chi_j (1 - \Phi_j)^2 \quad (26)$$

where  $\Phi_j$  is the volume fraction of a volatile component  $j$ ;  $\chi_j$ , the Flory interaction parameter; and  $m_j$ , the ratio of molar volumes of the polymer and solvent (volatiles). Since the amounts of volatile species in the polymer melt phase are very small at a high reaction temperature and low pressure (vacuum) (i.e.,  $\Phi_j \ll 1$ ), the Flory–Huggins equation is reduced to

$$\gamma_j = \frac{1}{m_j} \exp \left( 1 - \frac{1}{m_j} + \chi_j \right) \quad (27)$$

The following equation is used to estimate the Flory interaction parameter  $\chi_j$  (ref. 6):

$$\chi_j = 0.34 + \frac{v_j}{RT} (\delta_j - \delta_{\text{poly}})^2 \quad (28)$$

where  $\delta_j$  and  $\delta_{\text{poly}}$  are the solubility parameters of component  $j$  and polycarbonate, respectively, and  $v_j$  is the liquid molar volume of component  $j$ . The numerical values of the solubility parameters and the liquid molar volumes are listed in Table I.

To calculate the vapor- and liquid-phase compositions and the amounts of volatile components removed from the reaction system, the following assumptions are made:

1. Thermodynamic phase equilibrium is quickly established in the reactor and the reflux column.

**Table I Solubility Parameter Data and Liquid Molar Volume Data of Phenol, DPC, and Polycarbonate<sup>7</sup>**

$\delta$ (phenol)	12.05 (cal <sup>1/2</sup> /cm <sup>3/2</sup> )
$\delta$ (DPC)	10.45 (cal <sup>1/2</sup> /cm <sup>3/2</sup> )
$\delta$ (polycarbonate)	9.94 (cal <sup>1/2</sup> /cm <sup>3/2</sup> )
$v$ (phenol)	$8.787 \times 10^{-2}$ (L/mol)
$v$ (DPC)	$1.684 \times 10^{-1}$ (L/mol)

2. Only phenol and DPC evaporate in the reactor.

With these assumptions, we can derive the following component balance equations:

$$F = G + L \quad (29)$$

$$y_B p_t = \gamma_B x_B P_B^{\text{sat}} \quad (30)$$

$$y_P p_t = \gamma_P x_P P_P^{\text{sat}} \quad (31)$$

$$F x_{AF} = L x_A \quad (32)$$

$$F x_{BF} = G y_B + L x_B \quad (33)$$

$$F x_{PF} = G y_P + L x_P \quad (34)$$

$$F x_{\text{poly},F} = L x_{\text{poly}} \quad (35)$$

$$x_{AF} + x_{BF} + x_{PF} + x_{\text{poly},F} = 1 \quad (36)$$

$$x_A + x_B + x_P + x_{\text{poly}} = 1 \quad (37)$$

$$y_B + y_P = 1 \quad (38)$$

where  $F$  is the total moles of the feed (in the liquid and vapor phases) before the flash separation, and  $L$  and  $G$ , the total moles of the liquid and vapor phases in the reactor after the flash separation.  $x_{AF}$ ,  $x_{BF}$ ,  $x_{PF}$ , and  $x_{\text{poly},F}$  are the mol fractions of two monomers, phenol, and the polymer, respectively, in the liquid phase before the flash separation.  $x_A$ ,  $x_B$ ,  $x_P$ , and  $x_{\text{poly}}$  are the corresponding mol fractions after the flash separation.  $y_B$  is the mol fraction of DPC in the vapor phase.

Equations (29)–(38) are reduced to the following four equations:

$$Fx_{AF} = Lx_A \quad (39)$$

$$Fx_{BF} = (F - L) \frac{\gamma_B x_B P_B^{\text{sat}}}{p_t} + Lx_B \quad (40)$$

$$Fx_{PF} = (F - L) \frac{\gamma_P x_P P_P^{\text{sat}}}{p_t} + Lx_P \quad (41)$$

$$F(1 - x_{AF} - x_{BF} - x_{PF}) = L(1 - x_A - x_B - x_P) \quad (42)$$

We can solve the above four nonlinear equations for four unknowns ( $L$ ,  $x_A$ ,  $x_B$ , and  $x_P$ ).

To calculate the amount of the condensed liquid refluxed to the reactor, the following equations are derived for the reflux column. Here, it is assumed that the reflux column is at a stationary state (i.e., at thermodynamic phase equilibrium):

$$Gy_B = V^*y_{B,S} + L^*x_{B,S} \quad (43)$$

$$Gy_P = V^*y_{P,S} + L^*x_{P,S} \quad (44)$$

$$y_{B,S}p_t = \gamma_{B,S}x_{B,S}P_B^{\text{sat}*} \quad (45)$$

$$y_{P,S}p_t = \gamma_{P,S}x_{P,S}P_P^{\text{sat}*} \quad (46)$$

$$G = V^* + L^* \quad (47)$$

$$y_{B,S} + y_{P,S} = y_B + y_P = x_{B,S} + x_{P,S} = 1 \quad (48)$$

where  $V^*$  is the molar flow rate of vapor leaving the reflux column, and  $L^*$ , the molar flow rate of condensed liquid from the reflux column to the reactor.  $P_B^{\text{sat}*}$  is the vapor pressure of DPC, and  $P_P^{\text{sat}*}$ , the saturated vapor pressure of phenol at the reflux column temperature.  $y_{B,S}$  and  $y_{P,S}$  are the mol fractions of DPC and phenol in the vapor phase, respectively.  $x_{B,S}$  is the mol fraction of DPC in the condensed liquid phase in the reflux column. Using eqs. (43)–(48), we obtain the following nonlinear equations:

$$Gy_B = (G - L^*) \frac{\gamma_{B,S}(1 - x_{P,S})P_B^{\text{sat}*}}{p_t} + L^*(1 - x_{P,S}) \quad (49)$$

$$Gy_P = (G - L^*) \frac{\gamma_{P,S}x_{P,S}P_P^{\text{sat}*}}{p_t} + L^*x_{P,S} \quad (50)$$

The activity coefficients of phenol ( $\lambda_{P,S}$ ) and DPC ( $\lambda_{B,S}$ ) are calculated using the Wilson equations<sup>8</sup>:

$$\ln \gamma_{P,S} = -\ln(x_{P,S} + x_{B,S}\Lambda_{PB}) + x_{B,S} \left( \frac{\Lambda_{PB}}{x_{P,S} + x_{B,S}\Lambda_{PB}} - \frac{\Lambda_{BP}}{x_{B,S} + x_{P,S}\Lambda_{BP}} \right) \quad (51)$$

$$\ln \gamma_{B,S} = -\ln(x_{B,S} + x_{P,S}\Lambda_{BP}) - x_{P,S} \left( \frac{\Lambda_{PB}}{x_{P,S} + x_{B,S}\Lambda_{PB}} - \frac{\Lambda_{BP}}{x_{B,S} + x_{P,S}\Lambda_{BP}} \right) \quad (52)$$

where

$$\ln \Lambda_{PB} = a_{PB} + b_{PB}/T + c_{PB} \ln T + d_{PB}T \quad (53)$$

$$\ln \Lambda_{BP} = a_{BP} + b_{BP}/T + c_{BP} \ln T + d_{BP}T \quad (54)$$

The binary parameters ( $a_{ij}$ ,  $b_{ij}$ ,  $c_{ij}$ , and  $d_{ij}$ ) in the above equations are determined by using the vapor–liquid equilibrium data regression package of *ASPEN Plus*®.

The volumetric evaporation rates of DPC,  $V_B$ , and phenol,  $V_P$ , are represented as follows:

$$V_B = (G - L^*) \frac{(1 - x_{P,S})P_B^{\text{sat}*}}{p_t} v_B \quad (55)$$

$$V_P = (G - L^*) \frac{x_{P,S}P_P^{\text{sat}*}}{p_t} v_P \quad (56)$$

where  $v_B$  and  $v_P$  are the molar volumes of DPC and phenol, respectively.

A computer-simulation program was developed to obtain the numerical solution of the kinetic modeling equations and the thermodynamic equilibrium equations. Figure 2 illustrates the computational procedure and the symbols used in the above equations.

## RESULTS AND DISCUSSION

The vapor–liquid equilibrium data for a binary mixture of phenol and DPC are shown in Figure 3, where  $x_1$  and  $y_1$  denote the weight fractions of phenol in the liquid phase and the vapor phase, respectively. It is seen that the amount of DPC in the vapor phase becomes quite small for the weight fraction of phenol larger than 0.4. This is because the vapor pressure of phenol is much

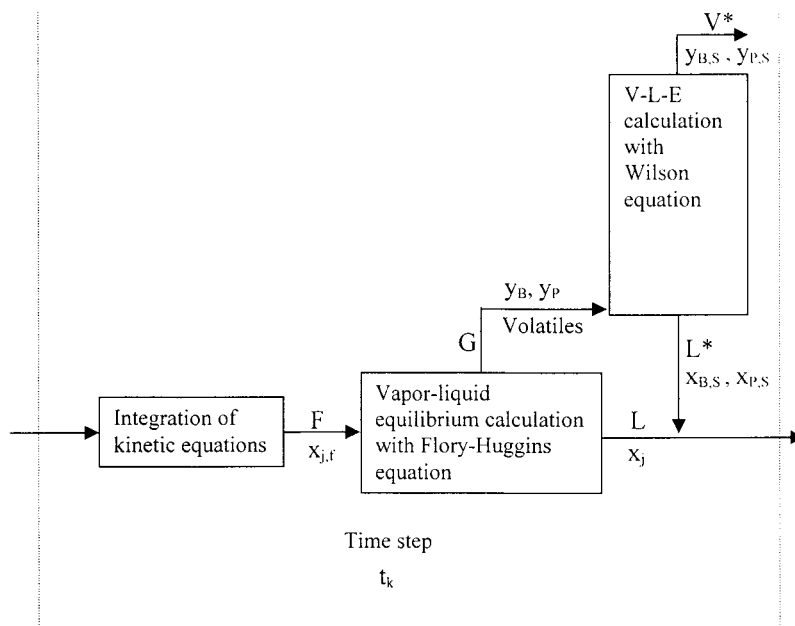


**Figure 2** Computational procedure for vapor–liquid composition in semibatch polymerization.

higher than that of DPC at the same temperature. The activity coefficients for phenol and DPC calculated using the vapor–liquid equilibrium data and the Wilson equation are plotted for varying weight fractions of phenol in the liquid phase in Figure 4. Notice that the activity coefficients,

particularly that of phenol, change significantly with the liquid-phase composition.

To investigate the effect of the initial mol ratio of DPC to BPA on the weight-average molecular weight of the polymer, we carried out semibatch polymerization experiments for seven different

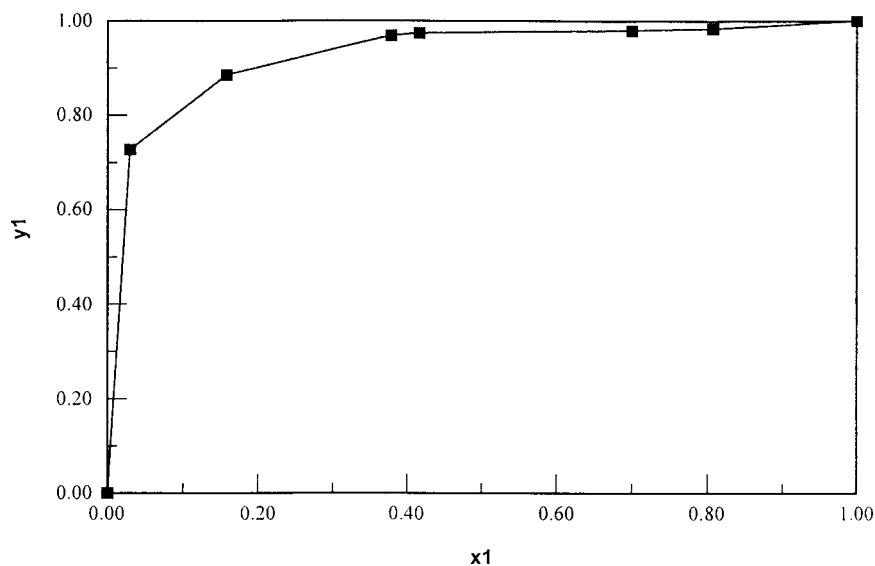


**Figure 3** Vapor–liquid equilibrium data for phenol–DPC system:  $x_1$  is the weight fraction of phenol in the liquid phase, and  $y_1$ , the weight fraction of phenol in the vapor phase.



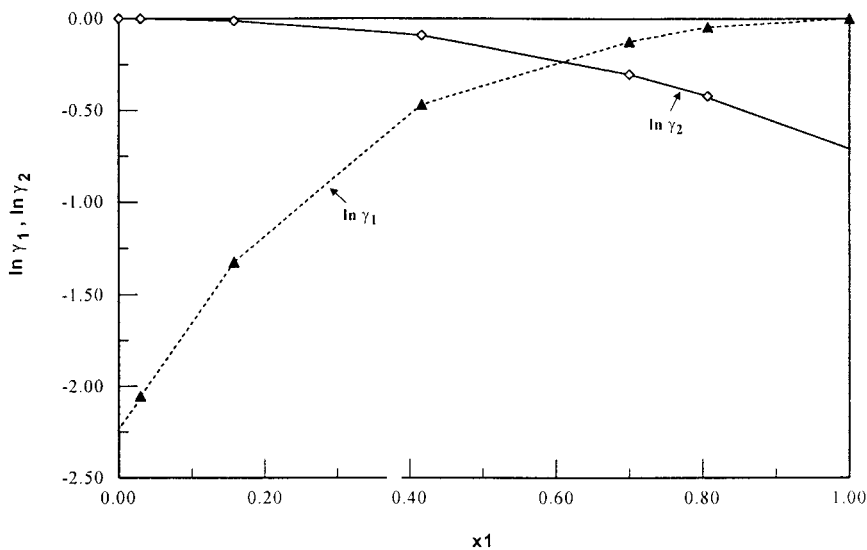


**Figure 4** Activity coefficients of (1) phenol and (2) DPC.

initial mol ratios (DPC/BPA). The reaction temperature was kept constant at 230°C. After the catalyst was injected into the reactor, the reaction pressure was reduced from ambient to 5 mmHg in 2 min. In these experiments, the catalyst concentration was  $8 \times 10^{-5}$  mol/L. The reflux column temperature was fixed at 82°C. Figure 5 shows the results of experiments and model simulations after 30 min of reaction time. It is observed that the experimental data are well fitted by the model and that the polymer molecular weight changes

significantly with the variation in the initial mol ratio. It is also seen that the highest molecular weight is obtained at the initial mol ratio of about 1.05. Theoretically, the highest molecular weight is obtainable when the concentrations of the two functional end groups are equal during the polymerization.

Figure 6 shows how the ratio of the hydroxyl end-group concentration to the carbonate end-group concentration changes with the reaction time. It is clearly seen that the ratio of the func-

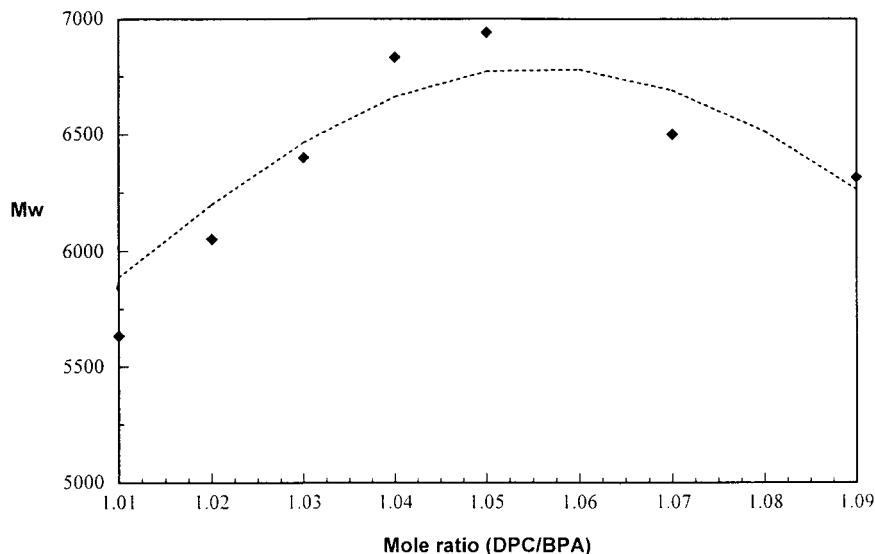


**Figure 5** Effect of initial monomer mol ratio on polymer molecular weight (230°C; 5 mmHg; reaction time, 30 min; reflux column temperature, 82°C).

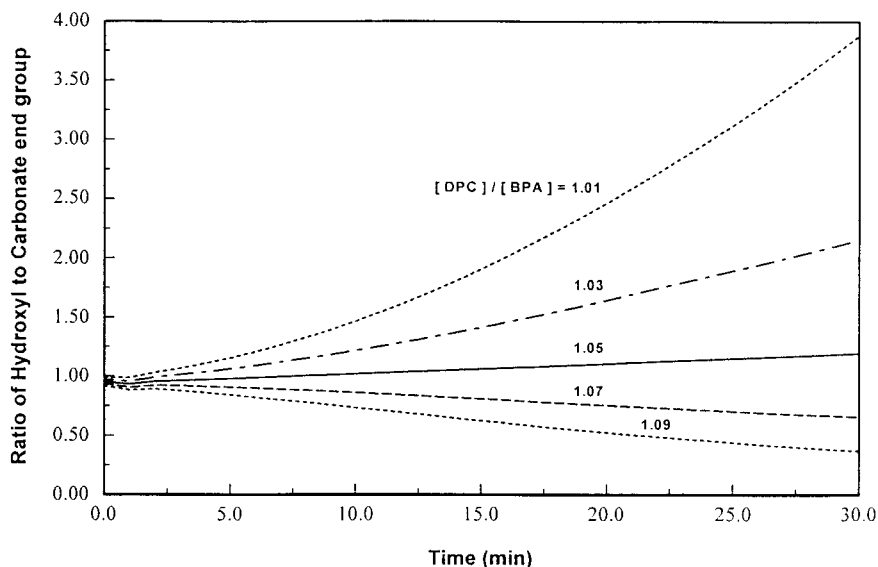


**Figure 6** Molar ratio of hydroxyl end group to carbonate end group versus reaction time (230°C; 5 mmHg; reflux column temperature, 82°C).

tional groups is almost unity when the initial DPC to BPA mol ratio is 1.05, at which the highest molecular weight is obtained. For other initial DPC/BPA mol ratios, the ratio of the two functional end-group concentrations deviate from unity as polymerization progresses. It is also interesting to note that the deviation becomes more significant as conversion increases for smaller values of the initial mol ratios, because more DPC

is lost during the polymerization at low DPC/BPA initial ratios than at higher DPC/BPA ratios when a high vacuum is applied.

Figure 7 shows the molecular weight profiles for 150 min of polymerization at 230°C with the initial DPC/BPC ratio of 1.02. The reflux column temperature is set at 82°C. The weight-average molecular weight of PC increases rapidly in the first 60 min but it levels off afterward. The solid

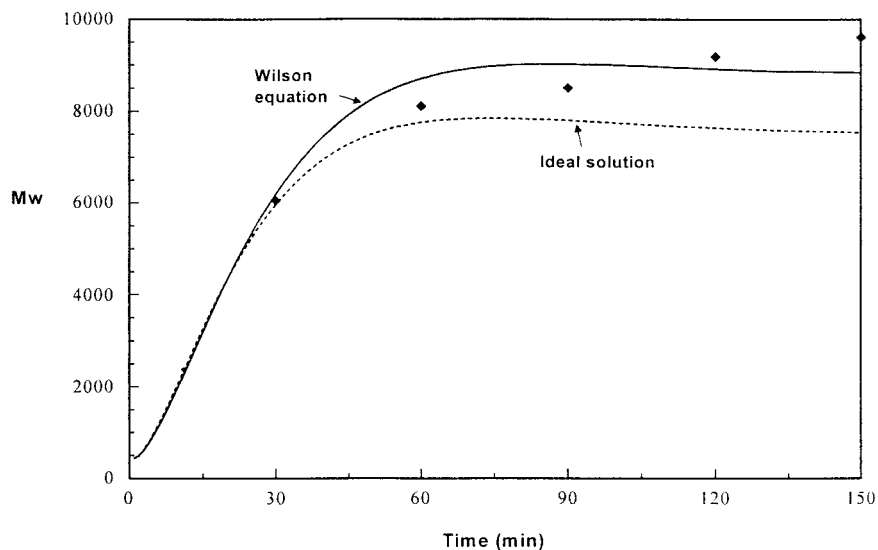


**Figure 7** Weight-average molecular weight versus reaction time [230°C; 5 mmHg; reflux column temperature, 82°C;  $(\text{DPC/BPA})_0 = 1.02$ ].

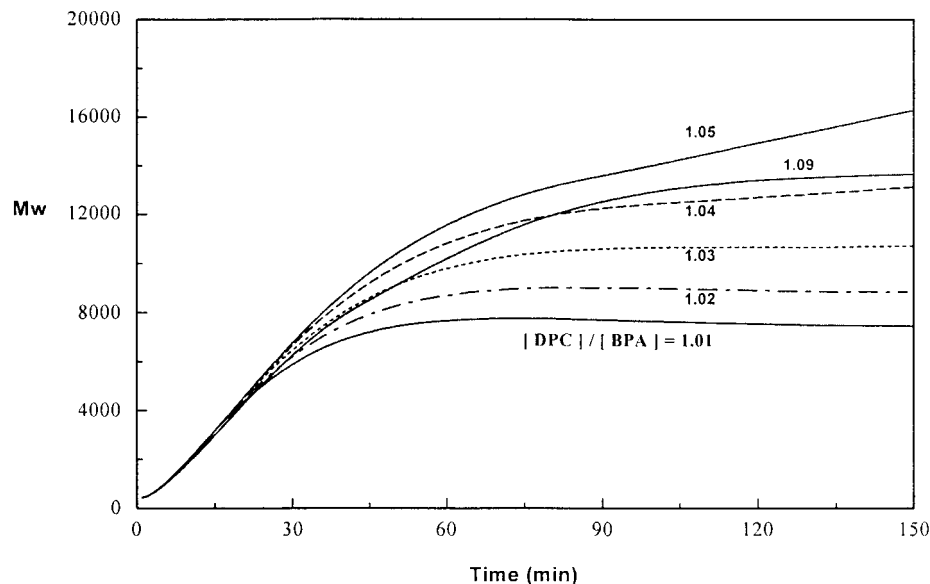


**Figure 8** Effect of initial DPC/BPA mol ratios on polymer molecular weight (230°C; 5 mmHg; reflux column temperature, 82°C).

line in Figure 7 represents the model simulation with the Wilson equation for vapor-liquid equilibrium calculations and the dotted line represents the simulation results when the ideal solution is assumed for the phenol-DPC mixture (i.e., activity coefficients are equal to 1.0). As expected, the use of an ideal solution model results in larger deviations from the experimental data. The

weight-average molecular weight values calculated for different initial DPC/BPA mol ratios are also shown in Figure 8. It is seen that the highest molecular weight is obtained when the initial mol ratio is 1.05. When the initial mol ratio is 1.01, the polymer molecular weight after 150 min is only 50% of the molecular weight when the initial mol ratio of 1.05 is used. It is also seen that the

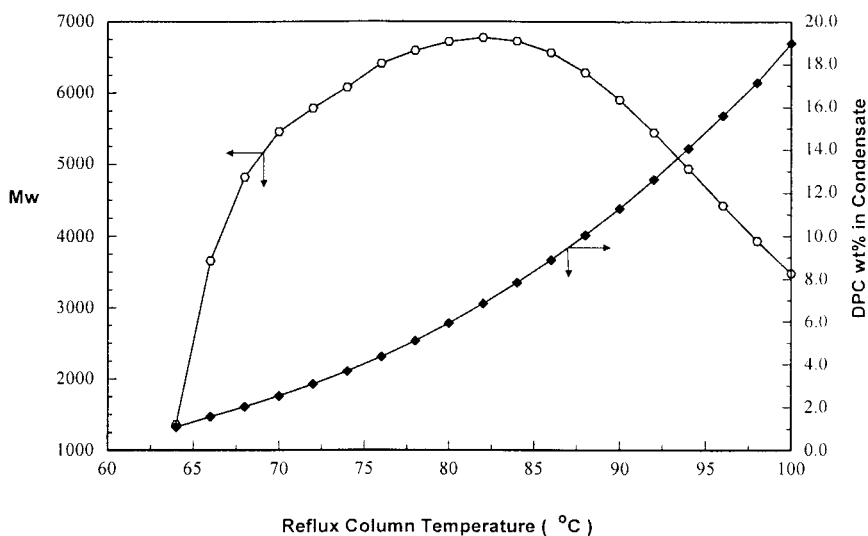


**Figure 9** Effect of reflux column temperature on the amount of DPC lost from the reactor and polymer molecular weight [230°C; 5 mmHg;  $(\text{DPC/BPA})_0 = 1.05$ ; reaction time, 30 min].

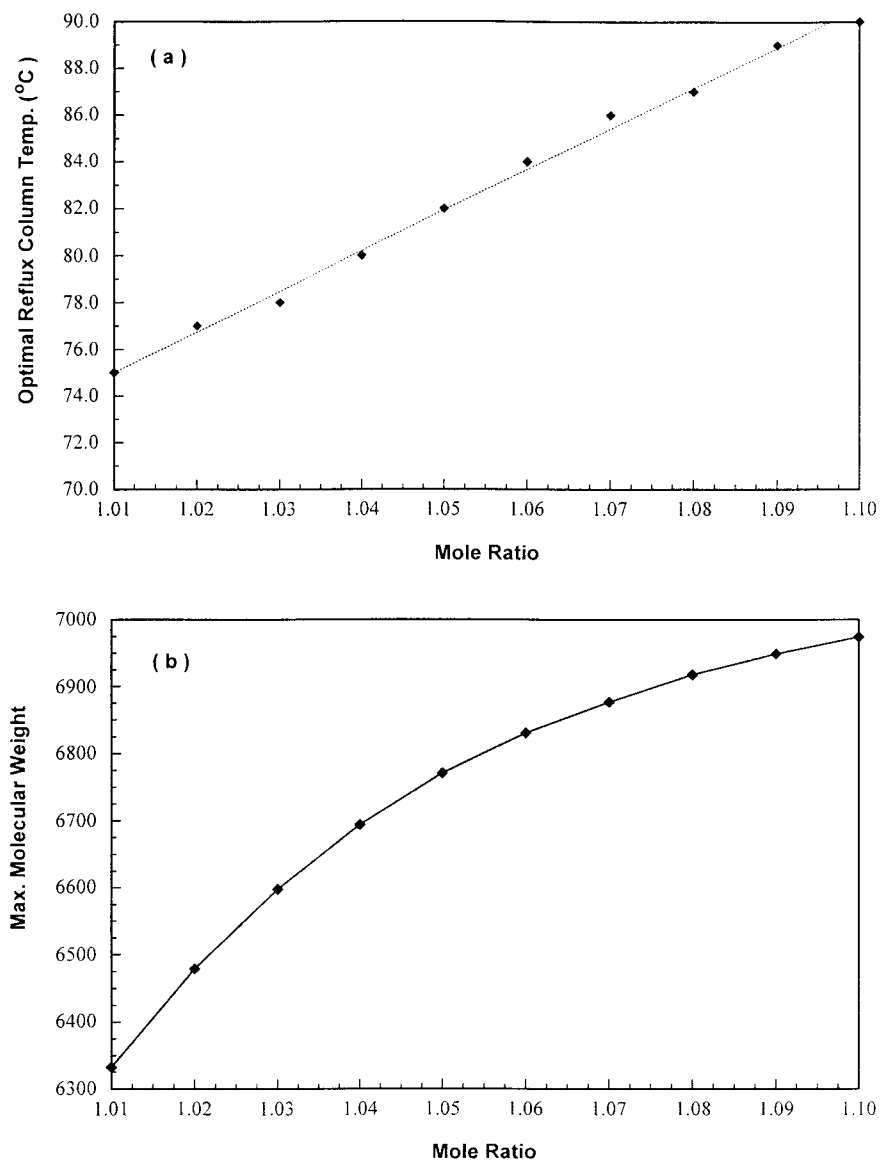


**Figure 10** (a) Calculated optimal reflux column temperature versus DPC/BPA mol ratio; (b) maximum molecular weight versus initial DPC/BPA mol ratio (reaction temperature, 230°C; 5 mmHg).

polymer molecular weight keeps increasing only when the ratio of the functional end groups is almost unity during the course of polymerization (e.g., initial DPC/BPA mol ratio is 1.05).

One of the most important objectives in our reaction modeling is to quantify the loss of DPC from the reaction system, particularly from the reflux column. In designing a reflux column or determining the reflux column operating conditions, the column temperature is the key factor. Figure 9 shows the effect of the reflux column temperature on the weight percent of DPC in the

condensate and the molecular weight of the polymer. Notice that the amount of DPC lost from the system and the resulting molecular weight are closely related to the reflux column temperature at a given reactor pressure and reaction temperature. For the initial DPC/BPA mol ratio of 1.05, Figure 9 indicates that the optimal reflux column temperature is about 82°C. We can also expect that a different optimal reflux column temperature may exist for different initial DPC/BPA mol ratios because the amount of DPC lost from the reaction system is strongly dependent on the re-

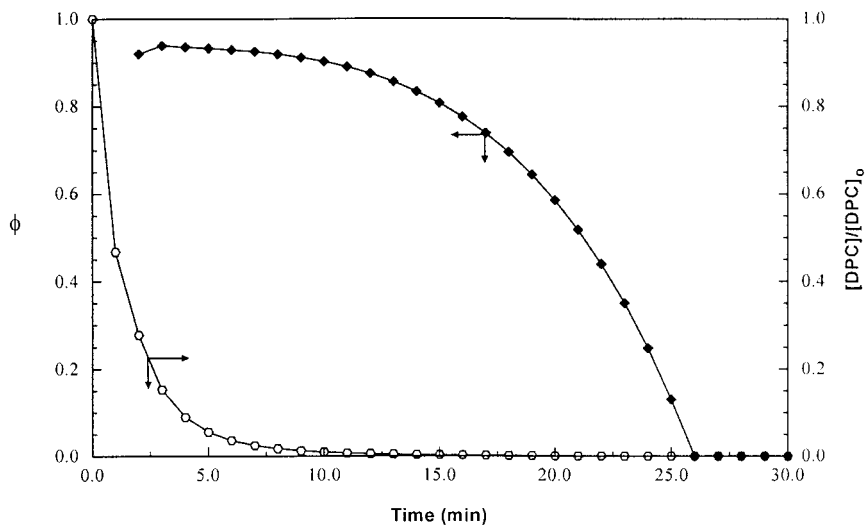


**Figure 11** Empirical reflux efficiency factor ( $\Phi$ ) and the change in the DPC concentration (230°C; 5 mmHg; reflux column temperature, 82°C).

flux column temperature. The calculated optimal reflux column temperatures for different initial DPC/BPA mol ratios are shown in Figure 10 (reaction temperature, 230°C). It is interesting to note that the optimal reflux column temperature is almost linearly proportional to the initial mono-

mer mol ratio. It is also seen that the higher the initial mol ratio is the higher the reflux column temperature needed to obtain high molecular weight.

In the previous work by Kim and Choi,<sup>3</sup> the amount of DPC refluxed to the reactor from the

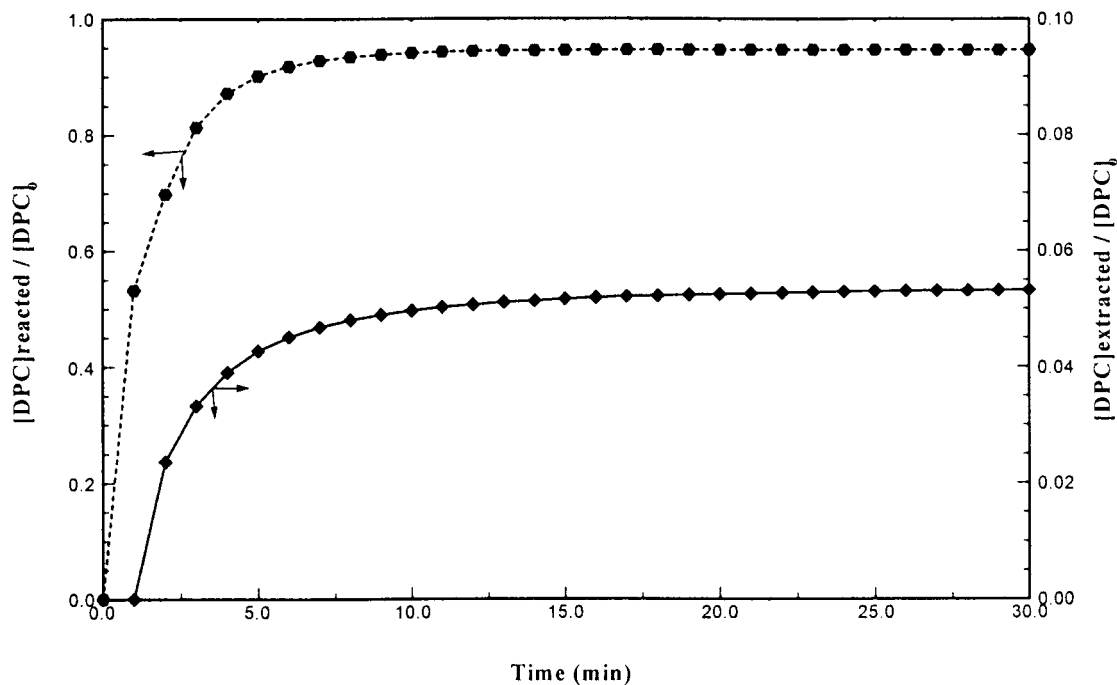


**Figure 12** Amounts of DPC consumed by reaction and removed from reactor through reflux column (230°C; 5 mmHg; reflux column temperature, 82°C).

reflux column was not calculated from the vapor–liquid equilibrium model. Instead, an empirical separation factor,  $\phi$ , was introduced as an adjustable parameter. The separation factor accounts for the fraction of DPC refluxed to the reactor from the reflux column and the constant separation factor was used for the entire period of polymerization. However, the amount of DPC refluxed to the reactor changes with conversion. Figure 11 illustrates the separation factor calculated from the vapor–liquid equilibrium model presented in this work. Notice that the separation factor seems to change significantly with the reaction time, particularly after about 10 min. However, Figure 12 shows that pure DPC is quickly consumed by the reaction in the first 8 min and about 5% of the initial DPC is removed from the reactor. In other words, the amount of DPC left after 10 min of reaction is very small and, thus, the rapidly decreasing reflux efficiency factor in Figure 11 has little practical significance. Therefore, one can assume that the reflux efficiency factor is nearly constant in the early reaction period in which the concentration of DPC changes rapidly.

## CONCLUSIONS

For quantitative modeling of a semibatch melt polycondensation of DPC and BPA, it is necessary to calculate the exact amount of monomers in the reactor during the entire course of polymerization. Since one of the monomers, DPC, exhibits an appreciable vapor pressure, a reflux column temperature needs to be set appropriately to keep the stoichiometric mol ratio of reactive end groups in the reactor during the polymerization. In this

work, a computational method is presented to calculate the exact amount of DPC returned back to the reactor from the reflux column using the vapor–liquid equilibrium model for a DPC–phenol binary mixture in the reflux column. It was observed that a slight excess amount of DPC should be used to maintain the stoichiometric mol ratio of the functional end groups and, hence, to obtain a high prepolymer molecular weight. It was also shown that the optimal reflux column temperature depends on the initial DPC/BPA mol ratio. The higher the ratio is, the higher the reflux column temperature that should be employed. The method presented in this work can be used to optimize the operating conditions of a reactor/reflux column system.

This work was supported by LG Chemical Co., Taejeon, South Korea.

## REFERENCES

1. Carroll, S. Market Rep 1999, Nov. 15.
2. Schnell, H. *Chemistry and Physics of Polycarbonate*; Interscience: New York, 1964.
3. Kim, Y. S.; Choi, K. Y. *J Appl Polym Sci* 1993, 49, 747–764.
4. *Dictionary of Organic Compounds*, 5<sup>th</sup> ed.; Buckingham, J., Ed.; Chapman & Hill: New York, 1982.
5. Flory, P. J. *Principles of Polymer Chemistry*; Cornell University: Ithaca, NY, 1953.
6. Ravindranath, K.; Mashelkar, R. A. *Chem Eng Sci* 1986, 41, 2197–2224.
7. Prausnitz, J. M. *Molecular Thermodynamics of Fluid-Phase Equilibria*; Prentice-Hall: New York, 1969.
8. Smith, J. M.; Van Ness, H. C. *Introduction to Chemical Engineering Thermodynamics*, 4<sup>th</sup> ed.; McGraw-Hill: New York, 1987.